Journal of Sound and Vibration (1999) **226**(4), 769–786
Article No. jsvi.1999.2313, available online at http://www.idealibrary.com on IDEAL®

FREE VIBRATION ANALYSIS OF RECTANGULAR PLATES WITH VARIOUSLY-SHAPED HOLES

M. HUANG

Graduate School of Marine Science and Engineering, Nagasaki University, Nagasaki 852 *Japan*

AND

T. SAKIYAMA

Department of Structural Engineering, Nagasaki University, Nagasaki 852 *Japan*

(*Received* 8 *October* 1998, *and in final form* 12 *April* 1999)

An approximate method for analyzing the free vibration of rectangular plates with a hole of different shapes is proposed. The shapes of the holes are circular, semi-circular, elliptic, square, rectangular, triangular, rhombic, etc. These rectangular plates with a hole can be considered ultimately as a kind of rectangular plates with non-uniform thickness. A hole in a plate can be considered as an extremely thin part of the plate. Therefore, the free vibration problem of a plate with a hole can be translated into the free vibration problem of the equivalent rectangular plate with non-uniform thickness. For some plates with different-shaped holes the convergency and accuracy of the numerical solutions calculated by the proposed method are investigated.

1. INTRODUCTION

Rectangular plates with a square, rectangular or circular hole are used in many types of civil, mechanical, marine or aeronautical structures to lighten the weight of a structure, to obtain the convenient connection of structural members or to change the resonant frequency of a member or structure. Therefore, the characteristics of free vibration of plates with an opening hole have been investigated for obtaining the design data of such structures.

Most previous investigations have been confined to plates with circular holes [1–3, 5], and square or rectangular holes [4, 6–8]. Further, in these studies the positions of holes were limited to the central part of the plates.

In this paper an approximate method for analyzing the free vibration of rectangular plates with an arbitrarily-located hole of different shapes is proposed by applying the discrete solution [9] for a rectangular plate with variable thickness. The shapes of the hole are circular, semi-circular, elliptic, square, rectangular, triangular and rhombic, etc. These rectangular plates with a hole can be considered ultimately as a kind of rectangular plates with non-uniform thickness. As a hole in

0022-460X/99/390769 + 18 $30.00/0

a plate can be considered as an extremely thin part of the plate, the free vibration problem of a plate with a hole can be translated into the free vibration problem of the equivalent rectangular plate with non-uniform thickness, and by applying the discrete Green function, the free vibration problem of the plate is translated into the eigenvalue problem. For some examples of plates with an arbitrarily located hole of different shapes, the convergency and accuracy of numerical solutions calculated by the proposed method are investigated, and much numerical data are obtained.

2. DISCRETE GREEN FUNCTION OF RECTANGULAR PLATE WITH ARBITRARILY VARIABLE THICKNESS

The Green function of a plate bending problem is given by the displacement function of the plate with a unit concentrated load. Thus, the Green function $w(x, y, x_q, y_r)/\bar{P}$ of a rectangular plate with arbitrarily variable thickness can be obtained from the fundamental differential equations of the plate with a concentrated load $\bar{P}$ at a point (x_q, y_r), which are given by following equations:

$$\frac{\partial Q_x}{\partial x} + \frac{\partial Q_y}{\partial y} + \bar{P}\delta(x - x_q)\delta(y - y_r) = 0, \qquad \frac{\partial M_y}{\partial y} + \frac{\partial M_{xy}}{\partial x} - Q_y = 0,$$

$$\frac{\partial M_x}{\partial x} + \frac{\partial M_{xy}}{\partial y} - Q_x = 0, \qquad \frac{\partial \theta_x}{\partial x} + v\frac{\partial \theta_y}{\partial y} = \frac{M_x}{D}, \qquad \frac{\partial \theta_y}{\partial y} + v\frac{\partial \theta_x}{\partial x} = \frac{M_y}{D},$$

$$\frac{\partial \theta_x}{\partial y} + \frac{\partial \theta_y}{\partial x} = \frac{2}{(1 - v)}\frac{M_{xy}}{D}, \qquad \frac{\partial w}{\partial x} + \theta_x = \frac{Q_x}{Gt_s}, \qquad \frac{\partial w}{\partial y} + \theta_y = \frac{Q_y}{Gt_s} \qquad \text{(1a–h)}$$

where Q_x, Q_y are the shearing forces, M_{xy} the twisting moment, M_x, M_y the bending moments, θ_x, θ_y the slopes, w the deflection, $D = Eh^3/12(1 - v^2)$ the bending rigidity, E, G the modulus and shear modulus of elasticity, respectively, v-Poisson's ratio, $h = h(x, y)$ the thickness of the plate, $t_s = h/12$, $\delta(x - x_q)$, $\delta(y - y_r)$ Dirac's delta functions.

By introducing the non-dimensional expressions

$$[X_1, X_2] = \frac{a^2}{D_0(1 - v^2)}[Q_y, Q_x], \qquad [X_3, X_4, X_5] = \frac{a}{D_0(1 - v^2)}[M_{xy}, M_y, M_x],$$

$$[X_6, X_7, X_8] = [\theta_y, \theta_x, w/a],$$

the differential equations (1a–h) are rearranged as follows:

$$\sum_{e=1}^{8}\left[F_{1te}\frac{\partial X_e}{\partial \zeta} + F_{2te}\frac{\partial X_e}{\partial \eta} + F_{3te}X_e\right] + P\delta(\eta - \eta_q)\delta(\zeta - \zeta_r)\delta_{1t} = 0, \qquad (2)$$

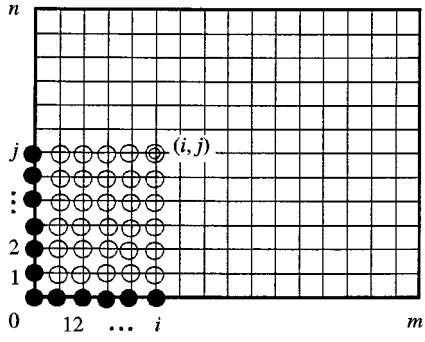

Figure 1. Discrete points on plate.

where $t = 1 \sim 8$, $\mu = b/a$, $\eta = x/a, \zeta = y/b$, $D_0 = Eh_0^3/12(1 - v^2)$ is the standard bending rigidity, h_0 the standard thickness of plate, a, b the breadth, length of the rectangular plate, $P = \bar{P}a/D_0(1 - v^2)$, δ_{ft} Kronecker's delta, and F_{1te}, F_{2te}, F_{3te} are given in Appendix A.

A rectangular plate divided vertically into m equal-length parts and horizontally into n equal-length parts as shown in Figure 1. The plate is considered as a group of discrete points which are intersections of the $(m + 1)$-vertical and $(n + 1)$-horizontal dividing lines. In this paper, the rectangular area, $0 \leqslant \eta \leqslant \eta_i$, $0 \leqslant \zeta \leqslant \zeta_j$, corresponding to the arbitrary intersection (i, j) as shown in Figure 1, is denoted as the area $[i, j]$. The intersection (i, j) denoted by ● is called the main point of the area, and the intersections denoted by ○ are called the inner-dependent points of the area, and the intersections denoted by ● are called the boundary-dependent points of the area.

By integrating equation (2) over the area $[i, j]$, the following integral equation is obtained:

$$\sum_{e=1}^{8} \left\{ \begin{aligned} & F_{1te} \int_0^{\eta_i} [X_e(\eta, \zeta_j) - X_e(\eta, 0)] \, d\eta + F_{2te} \int_0^{\zeta_j} [X_e(\eta_i, \zeta) - X_e(0, \zeta)] \, d\zeta \\ & + F_{3te} \int_0^{\eta_i} \int_0^{\zeta_j} X_e(\eta, \zeta) \, d\eta \, d\zeta \end{aligned} \right\}$$

$$+ Pu(\eta - \eta_q) u(\zeta - \zeta_r) \delta_{1t} = 0, \tag{3}$$

where $u(\eta - \eta_q)$, $u(\zeta - \zeta_r)$ are unit step functions.

Next, by applying the numerical integration method, the simultaneous equation for the unknown quantities $X_{eij} = X_e(\eta_i, \zeta_j)$ at the main point (i, j) of the area $[i, j]$ is obtained as follows:

$$\sum_{e=1}^{8} \left\{ F_{1te} \sum_{k=0}^{i} \beta_{ik} (X_{ekj} - X_{ek0}) + F_{2te} \sum_{l=0}^{j} \beta_{jl} (X_{eil} - X_{e0l}) + F_{3te} \sum_{k=0}^{i} \sum_{l=0}^{j} \beta_{ik} \beta_{jl} X_{ekl} \right\}$$

$$+ Pu_{iq} u_{jr} \delta_{1t} = 0, \tag{4}$$

where

$$u_{iq} = \begin{cases} 0 & (i<q), \\ 0{\cdot}5 & (i=q), \\ 1 & (i>q), \end{cases} \qquad u_{jr} = \begin{cases} 0 & (j<r), \\ 0{\cdot}5 & (j=r), \\ 1 & (j>r), \end{cases} \qquad \alpha_{ik} = \begin{cases} 0{\cdot}5 & (k=0,i), \\ 1 & (k\neq 0,i), \end{cases}$$

$$\alpha_{jl} = \begin{cases} 0{\cdot}5 & (l=0,j), \\ 1 & (l\neq 0,j), \end{cases} \qquad \beta_{ik} = \alpha_{ik}/m, \qquad \beta_{jl} = \alpha_{jl}/n.$$

The solution X_{pij} of the simultaneous equation (4) is obtained as follows:

$$X_{pij} = \sum_{e=1}^{8} \begin{cases} \sum_{k=0}^{i} \beta_{ik} A_{pe} [X_{ek0} - X_{ekj}(1-\delta_{ki})] + \sum_{l=0}^{j} \beta_{jl} B_{pe} [X_{e0l} - X_{eil}(1-\delta_{lj})] \\ + \sum_{k=0}^{i} \sum_{l=0}^{j} \beta_{ik}\beta_{jl} C_{pekl} X_{ekl} (1-\delta_{ki}\delta_{lj}) \end{cases} \tag{5}$$

$$- A_{p1} P u_{iq} u_{jr},$$

where $p = 1, 2, \ldots, 8$, $i = 1, 2, \ldots, m$, $j = 1, 2, \ldots, n$, and A_{pe}, B_{pe}, C_{pekl} are given in Appendix B.

In equation (5), the quantity X_{pij} at the main point (i, j) of the area $[i, j]$ is related to the quantities X_{ek0} and X_{e0l} at the boundary-dependent points of the area and the quantities X_{ekj}, X_{eil} and X_{ekl} at the inner-dependent points of the area. With the spreading of the area $[i, j]$ according to the regular order $[1, 1]$, $[1, 2], \ldots, [1, n]$, $[2, 1]$, $[2, 2], \ldots, [2, n], \ldots, [m, 1]$, $[m, 2], \ldots, [m, n]$, a main point of smaller area becomes one of the inner-dependent points of the following larger areas. Whenever the quantity X_{pij} at the main point (i, j) is obtained using equation (5) in the above-mentioned order, the quantities X_{ekj}, X_{eil} and X_{ekl} at the inner-dependent points of the following larger areas are eliminated by substituting the results obtained in the corresponding terms of the right-hand side of equation (5). By repeating this process, the equation X_{pij} at the main point is related to only the quantities X_{vk0}, $(v = 1, 3, 4, 6, 7, 8)$ and X_{s0l}, $(s = 2, 3, 5, 6, 7, 8)$ which are six independent quantities at each of the boundary-dependent points along the horizontal axis and the vertical axis in Figure 1 respectively. The results are as follows:

$$X_{pij} = \sum_{k=0}^{i} \left\{ \begin{array}{l} a_{1pijk1}(Q_y)_{k0} + a_{1pijk2}(M_{xy})_{k0} + a_{1pikj3}(M_y)_{k0} \\ + a_{1pijk4}(\theta_y)_{k0} + a_{1pijk5}(\theta_x)_{k0} + a_{1pijk6}(w)_{k0} \end{array} \right\}$$

$$+ \sum_{l=0}^{j} \left\{ \begin{array}{l} a_{2pijl1}(Q_x)_{0l} + a_{2pijl2}(M_{xy})_{0l} + a_{2pijl3}(M_x)_{0l} \\ + a_{2pijl4}(\theta_y)_{0l} + a_{2pijl5}(\theta_x)_{0l} + a_{2pijl6}(w)_{0l} \end{array} \right\} + \bar{q}_{pij} P, \tag{6}$$

where $(Q_y) = X_1$, $(Q_x) = X_2$, $(M_{xy}) = X_3$, $(M_y) = X_4$, $(M_x) = X_5$, $(\theta_y) = X_6$, $(\theta_x) = X_7$, $(w) = X_8$, and $a_{1pijk1}, \ldots, a_{2pijl6}$, $\bar{q}_{pij}$ are given in Appendix C. From equation (6), the discrete Green function of a rectangular plate with variable thickness is obtained from $X_{8ij} = G(x_i, y_j, x_q, y_r)$. $[\bar{P}a/D_0(1 - \nu^2)]$ which is the displacement at a point (x_i, y_j) of a plate with a concentrated load $\bar{P}$ at a point (x_q, y_r).

3. INTEGRAL CONSTANT AND BOUNDARY CONDITION OF RECTANGULAR PLATE

The integral constants $(Q_y)_{k0}, (M_{xy})_{k0}, \ldots, (w)_{k0}$, $(Q_x)_{0l}$, $(M_{xy})_{0l}, \ldots, (w)_{0l}$ being involved in the discrete solution (6) are to be evaluated by the boundary conditions of a rectangular plate. The combinations of the integral constants and the boundary conditions for three cases are shown in Figures 2–4, in which the integral constants and the boundary conditions at the four corners are shown in the boxes. The integral constants and the boundary conditions along the four edges are given at the equally spaced discrete points. In this paper simply supported, fixed and free edges are denoted by solid line ——, thick solid line —— and dotted line ..... and each plate in Figure 2, Figure 3 and Figure 4 by ssss, cccc and fsfs plates respectively.

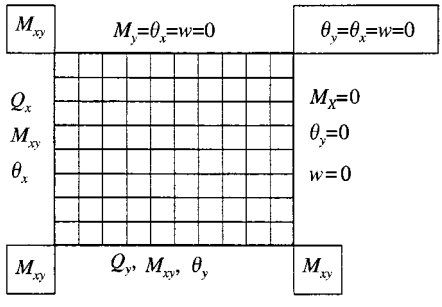

Figure 2. Simply supported plate.

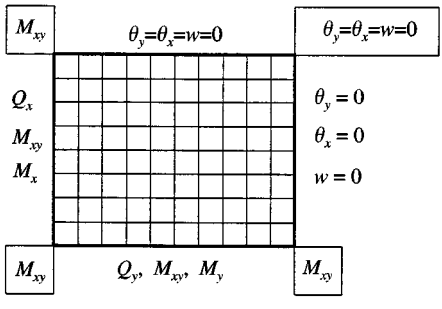

Figure 3. Fixed plate.

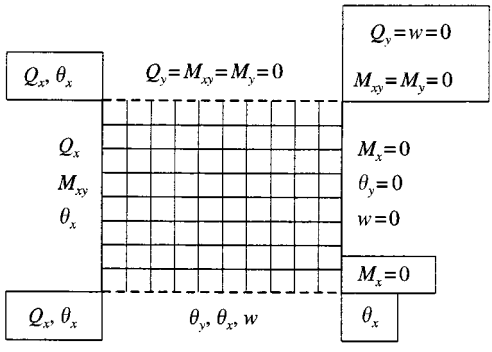

Figure 4. Plate with simple opposite edges and the other free edges.

4. EQUIVALENT RECTANGULAR PLATE OF PLATE WITH HOLE OF DIFFERENT SHAPES

Rectangular plates with a different-shaped hole —— circular, semi-circular, elliptic, square, rectangular, triangular or rhombic —— can be translated into their equivalent rectangular plates with non-uniform thickness by considering the hole to be an extremely thin part of the plate.

The thickness of the actual part of an original rectangular plate is expressed by h_0, and the thickness of an extremely thin part of the equivalent rectangular plate is expressed by h in this paper. The thickness of the equivalent rectangular plate varies discontinuously on the boundary line between the original actual part and the translated extremely thin part. An example of translation from an original plate with a hole to its equivalent rectangular plate with non-uniform thickness is shown in Figure 5, and the thickness h at each intersection marked by ■ of the extremely thin part of the equivalent rectangular plate which is inside the hole of the original plate is taken as $h \ll h_0$ as shown in the numerical work.

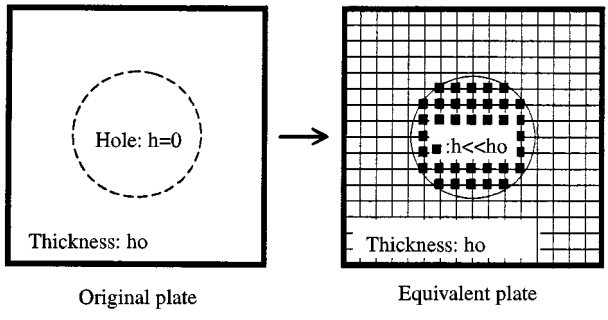

Figure 5. Example of equivalent plate.

5. CHARACTERISTIC EQUATION OF FREE VIBRATION OF PLATE WITH HOLE OF DIFFERENT SHAPES

By applying the Green function $w(x_0, y_0, x, y)/\bar{P}$ which is the displacement at a point (x_0, y_0) of a plate with a concentrated load $\bar{P}$ at a point (x, y), the

displacement amplitude $\hat{w}(x_0, y_0)$ at a point (x_0, y_0) of the equivalent rectangular plate during the free vibration is given as follows:

$$\hat{w}(x_0, y_0) = \int_0^b \int_0^a \rho h \omega^2 \hat{w}(x, y) [w(x_0, y_0, x, y)/\bar{P}] \, dx \, dy, \tag{7}$$

where ρ is the mass density of the plate material.

Using the non-dimensional expressions

$$\lambda^4 = \frac{\rho_0 h_0 \omega^2 a^4}{D_0(1 - v^2)}, \qquad H(\eta, \zeta) = \frac{\rho(x, y)}{\rho_0} \frac{h(x, y)}{h_0}, \qquad W(\eta, \zeta) = \frac{\hat{w}(x, y)}{a},$$

$$G(\eta_0, \zeta_0, \eta, \zeta) = \frac{w(x_0, y_0, x, y)}{a} \frac{D_0(1 - v^2)}{\bar{P}a}, \qquad \rho_0: \text{standard mass density},$$

the integral equation (7) can be rewritten as follows:

$$W(\eta_0, \zeta_0) = \int_0^1 \int_0^1 \mu \lambda^4 H(\eta, \zeta) G(\eta_0, \zeta_0, \eta, \zeta) W(\eta, \zeta) \, d\eta \, d\zeta. \tag{8}$$

By applying the numerical integration method, by equation (8) is discretely expressed as

$$\kappa W_{kl} = \sum_{i=0}^{m} \sum_{j=0}^{n} \beta_{mi} \beta_{nj} H_{ij} G_{klij} W_{ij}, \qquad \kappa = 1/(\mu \lambda^4). \tag{9}$$

From equation (9) homogeneous linear equations in $(m + 1) \times (n + 1)$ unknowns $W_{00}, W_{01}, \ldots, W_{0n}, W_{10}, W_{11}, \ldots, W_{1n}, \sim, W_{m0}, W_{m1}, \ldots, W_{mn}$ are obtained as follows:

$$\sum_{i=0}^{m} \sum_{j=0}^{n} (\beta_{mi} \beta_{nj} H_{ij} G_{klij} - \kappa \delta_{ik} \delta_{jl}) W_{ij} = 0 \quad (k = 0, 1, \ldots, m, l = 0, 1, \ldots, n). \tag{10}$$

The characteristic equation of the free vibration of the equivalent rectangular plate is obtained from equation (10) as follows:

$$\begin{vmatrix} \mathbf{K}_{00} & \mathbf{K}_{01} & \mathbf{K}_{02} & \cdots & \mathbf{K}_{0m} \\ \mathbf{K}_{10} & \mathbf{K}_{11} & \mathbf{K}_{12} & \cdots & \mathbf{K}_{1m} \\ \mathbf{K}_{20} & \mathbf{K}_{21} & \mathbf{K}_{22} & \cdots & \mathbf{K}_{2m} \\ & \cdots & & \cdots & \\ \mathbf{K}_{m0} & \mathbf{K}_{m1} & \mathbf{K}_{m2} & \cdots & \mathbf{K}_{mm} \end{vmatrix} = 0, \tag{11}$$

where

$$\mathbf{K}_{ij} = \beta_{mj} \begin{bmatrix} \beta_{n0}H_{j0}G_{i0j0} - \kappa\delta_{ij} & \beta_{n1}H_{j1}G_{i0j1} & \beta_{n2}H_{j2}G_{i0j2} & \cdots & \beta_{nn}H_{jn}G_{i0jn} \\ \beta_{n0}H_{j0}G_{i1j0} & \beta_{n1}H_{j1}G_{i1j1} - \kappa\delta_{ij} & \beta_{n2}H_{j2}G_{i1j2} & \cdots & \beta_{nn}H_{jn}G_{i1jn} \\ \beta_{n0}H_{j0}G_{i2j0} & \beta_{n1}H_{j1}G_{i2j1} & \beta_{n2}H_{j2}G_{i2j2} - \kappa\delta_{ij} & \cdots & \beta_{nn}H_{jn}G_{i2jn} \\ & \cdots & \cdots & & \\ \beta_{n0}H_{j0}G_{inj0} & \beta_{n1}H_{j1}G_{inj1} & \beta_{n2}H_{j2}G_{inj2} & \cdots & \beta_{nn}H_{jn}G_{injn} - \kappa\delta_{ij} \end{bmatrix}$$

6. NUMERICAL WORK

The convergency and accuracy of numerical solutions have been investigated for the free vibration problem of some rectangular plates with a different-shaped hole circular, semi-circular, elliptic, square, rectangular, triangular or rhombic —— as shown in Figure 6 (a)–(h). The numerical solutions for the natural frequency parameters of these plates have been obtained for the case of aspect ratio $b/a = 1$ and Poisson's ratio $v = 0{\cdot}3$ using Richardson's extrapolation formula for the two cases of divisional numbers m $(= n)$.

6.1. CONVERGENCY AND ACCURACY OF NUMERICAL RESULTS FOR PLATES WITH HOLE

6.1.1. *Thin ssss square plate with square hole*

To examine the convergency of numerical values for the natural frequency parameter λ obtained from the proposed method, and determine the suitable values of the thickness ratio h/h_0 of the extremely thin part thickness h and actual part thickness h_0 and the divisional numbers *m and n*, the lowest 12 natural frequency

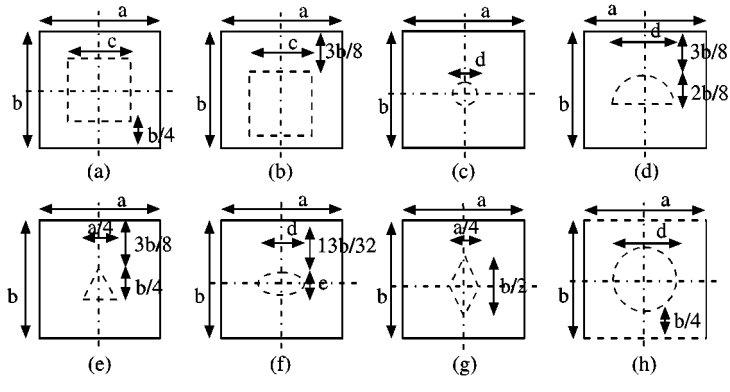

Figure 6. Rectangular plates with holes of different shapes.

parameters for the ssss square plates with a square hole of size ratio $c/a = 0{\cdot}5$ shown in Figures 6(a) and (b) were analyzed. The thickness h_0/a of these plates is 0·01. The results are shown in Figures 7 and 8. These show good convergency of the numerical solutions by the proposed method. After studying the curves of Figures 7 and 8, it was decided to set the thickness ratio $h/h_0 = 0{\cdot}1$ and the combination of the divisional number applying Richardson's extrapolation formula, $m(= n)$, at 12 and 16.

Numerical values for the lowest 12 natural frequency parameter λ of the ssss square plates with a square hole of size ratio $c/a = 0{\cdot}5$ at the central or lower part shown in Figures 6(a) and (b) are given in Table 1. Table 1 contains the other theoretical value by Ali and Atwal [7], and it shows the sufficient accuracy of the numerical solutions obtained by the present method. The nodal patterns of the 12 modes of the two plates are shown in Figure 9.

6.1.2. *Moderately thick ssss square plate with square hole*

Numerical solutions for the lowest 12 natural frequency parameters λ of the ssss square plate with a moderate thickness of $h_0/a = 0{\cdot}2$ and a square hole of size ratio $c/a = 0{\cdot}5$ at the central part shown in Figure 6(a) are given in Table 2. Table 2 contains the other theoretical value of the fundamental frequency in Reddy [8], and it shows the adequate accuracy of the numerical solutions obtained by the present method. The nodal patterns of the 12 modes of the plate are shown in Figure 10.

6.1.3. *Cccc square plate with circular hole*

Numerical solutions for the lowest 12 natural frequency parameters λ of the cccc square plate with a circular hole of size ratio $d/a = 0{\cdot}2$ at the central part shown in Figure 6(c) are given in Table 3. The thickness h_0/a of the plate is 0·01. Table 3

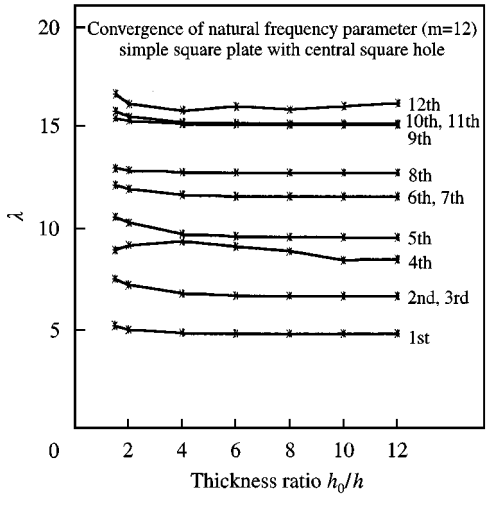

Figure 7. Convergency of natural frequency parameter ($m = 12$).

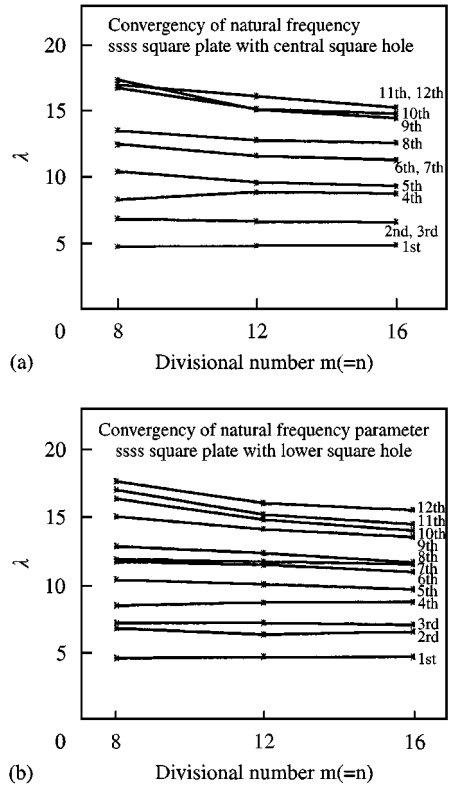

Figure 8. Convergency of natural frequency parameter ($h/h_0 = 0{\cdot}1$).

TABLE 1

Natural frequency parameter λ for ssss square plates with square hole

Mode	Central hole				Lower hole		
	m		Extraplation	References	*m*		Extrapolation
	12	16		[7]	12	16	
1	4·731	4·779	4·839	4·936	4·713	4·663	4·600
2	6·595	6·525	6·435	6·502	6·377	6·591	6·867
3	6·595	6·527	6·440	6·502	7·234	7·078	6·878
4	8·818	8·676	8·492	8·525	8·751	8·745	8·738
5	9·531	9·244	8·875	8·813	10·080	9·668	9·138
6	11·552	11·225	10·805	—	11·526	10·952	10·213
7	11·552	11·237	10·831	—	12·387	11·682	10·776
8	12·757	12·553	12·291	—	11·781	11·519	11·182
9	15·112	14·422	13·534	—	14·181	13·555	12·749
10	16·136	15·249	14·108	—	14·875	14·020	12·920
11	15·174	14·763	14·234	—	15·268	14·494	13·499
12	15·174	14·769	14·247	—	16·113	15·559	14·848

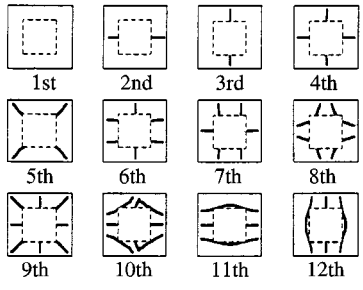

(a) Plate with central hole

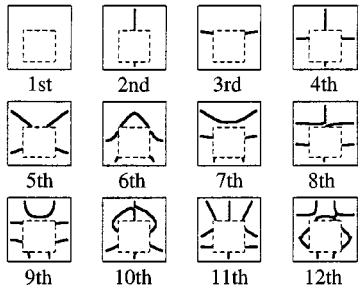

(b) Plate with lower hole

Figure 9. Nodal patterns for ssss square plate with square hole.

TABLE 2

Natural frequency parameter λ for ssss moderately thick square plate with central square hole ($h_0/a = 0{\cdot}2$)

Mode	m		Extrapolation	Reference [8]
	12	16		
1	4·533	4·574	4·628	4·753
2	5·775	5·792	5·814	—
3	5·775	5·792	5·814	—
4	7·731	7·486	7·329	—
5	7·579	7·501	7·401	—
6	9·065	8·964	8·833	—
7	9·065	8·964	8·833	—
8	10·032	9·884	9·694	—
9	10·886	10·601	10·235	—
10	11·341	11·105	10·802	—
11	11·341	11·105	10·802	—
12	12·249	11·691	11·333	—

contains the other theoretical value in Kumai [1], and it shows the sufficient accuracy of the numerical solutions obtained by the present method. The nodal patterns of the 12 modes of the plate are shown in Figure 11.

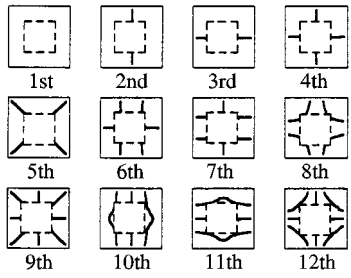

Figure 10. Nodal patterns for ssss moderately thick square plate with square hole.

TABLE 3

Natural frequency parameter λ for cccc square plate with central circular hole ($d/a = 0{\cdot}2$)

Mode	m		Extrapolation	Reference [1]
	12	16		
1	6·188	6·211	6·240	6·099
2	8·943	8·731	8·457	8·396
3	8·940	8·731	8·462	—
4	11·033	10·683	10·233	—
5	12·157	11·965	11·719	—
6	12·747	12·551	12·299	12·008
7	13·718	13·420	13·037	—
8	13·715	13·420	13·041	—
9	16·459	16·007	15·426	—
10	16·505	15·215	13·556	—
11	16·503	15·215	13·560	—
12	17·626	16·802	15·741	—

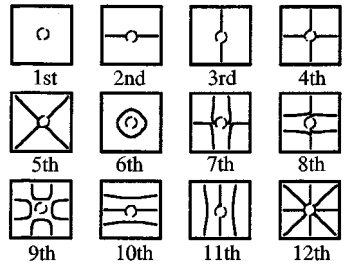

Figure 11. Nodal patterns for cccc square plate with central circular hole ($d/a = 0{\cdot}2$).

6.2. NUMERICAL RESULTS FOR PLATES WITH HOLE

6.2.1. *Ssss square plate with semi-circular hole*

Numerical solutions for the lowest 12 natural frequency parameters λ of the ssss square plates with a semi-circular hole of size ratio $d/a = 1/2$ at the central part

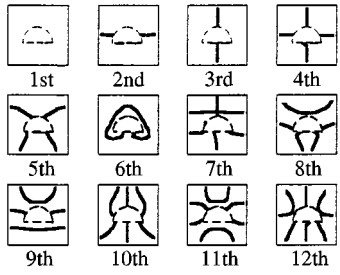

Figure 12. Nodal patterns for ssss square plate with semi-circular hole.

TABLE 4

Natural frequency parameter λ for ssss square plate with semi-circular hole

Mode	m		Extrapolation
	12	16	
1	4·522	4·532	4·545
2	6·666	6·568	6·416
3	7·027	7·005	6·977
4	8·988	8·947	8·893
5	10·194	9·927	9·584
6	11·568	11·083	10·459
7	11·904	11·578	11·160
8	11·630	11·559	11·466
9	13·188	13·048	12·868
10	14·159	13·719	13·154
11	14·924	14·481	13·910
12	15·480	14·844	14·027

shown in Figure 6(d) are given in Table 4. The thickness h_0/a of the plate is 0·01. The nodal patterns of the 12 modes of the plate as shown in Figure 12.

6.2.2. *Ssss square plate with triangular hole*

Numerical solutions for the lowest 12 natural frequency parameters λ of the ssss square plate with a triangular hole at the central part shown in Figure 6(e) are given in Table 5. The thickness h_0/a of the plate is 0·01. The nodal patterns of the 12 modes of the plates are shown in Figure 13.

6.2.3. *Ssss square plate with elliptic hole*

Numerical solutions for the lowest 12 natural frequency parameters λ of the ssss square plate with an elliptic hole of size ratio $d/a = 3/8$ and $d/e = 2$ at the central part shown in Figure 6(f) are given in Table 6. The thickness h_0/a of these plates is 0·01. The nodal patterns of the 12 modes of the three plates are shown in Figure 14.

TABLE 5

Natural frequency parameter λ for ssss square plate with triangular hole

Mode	m		Extrapolation
	12	16	
1	4·455	4·482	4·517
2	7·311	7·265	7·207
3	7·254	7·241	7·225
4	9·191	9·161	9·122
5	10·684	10·367	9·959
6	10·462	10·298	10·088
7	12·061	11·850	11·579
8	12·031	11·860	11·640
9	14·478	13·888	13·129
10	14·212	13·770	13·202
11	14·434	14·024	13·497
12	15·527	14·860	14·002

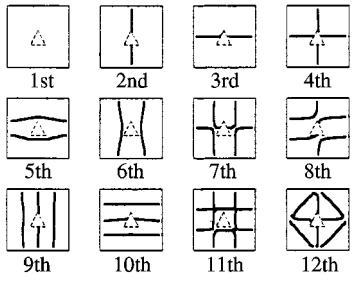

Figure 13. Nodal patterns for ssss square plate with triangular hole.

TABLE 6

Natural frequency parameter λ for ssss square plate with elliptic hole

Mode	m		Extrapolation
	12	16	
1	4·510	4·482	4·447
2	6·980	6·912	6·824
3	7·086	7·103	7·125
4	9·053	8·721	8·295
5	10·233	10·200	10·159
6	11·451	10·889	10·167
7	11·754	11·457	11·074
8	13·698	12·777	11·593
9	11·823	11·780	11·724
10	14·095	13·720	13·238
11	14·942	14·381	13·659
12	15·404	14·794	14·010

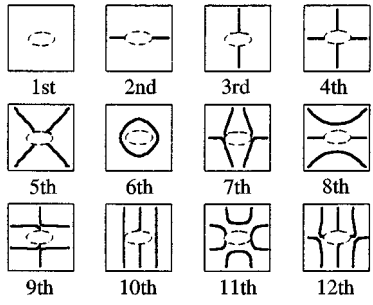

Figure 14. Nodal patterns for ssss square plate with elliptic hole.

TABLE 7

Natural frequency parameter λ for ssss square plate with rhombic hole

Mode	m		Extrapolation
	12	16	
1	4·628	4·547	4·442
2	7·332	7·138	6·889
3	7·442	7·276	7·062
4	9·176	9·145	9·106
5	10·467	10·239	9·947
6	11·565	10·996	10·264
7	11·982	11·651	11·225
8	12·232	11·888	11·446
9	14·778	13·502	11·862
10	14·925	14·076	12·983
11	15·195	14·456	13·505
12	15·496	14·950	14·249

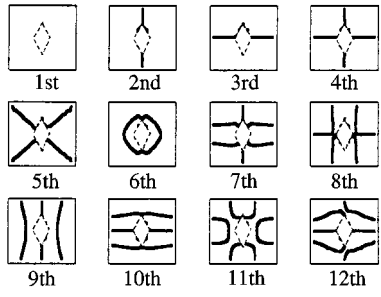

Figure 15. Nodal patterns for ssss square plate with rhombic hole.

6.2.4. *Ssss square plate with rhombic hole*

Numerical solutions for the lowest 12 natural frequency parameters λ of the ssss square plate with a rhombic hole at the central part shown in Figure 6(g) are given in Table 7. The thickness h_0/a of the plate is 0·01. The nodal patterns of the 12 modes of the plate are shown in Figure 15.

TABLE 8

Natural frequency parameter λ for fsfs square plate with circular hole

Mode	m		Extrapolation
	12	16	
1	3·299	3·036	2·699
2	4·308	4·233	4·137
3	6·231	5·880	5·428
4	6·975	6·865	6·724
5	7·263	7·096	6·881
6	9·257	8·849	8·324
7	9·124	8·793	8·367
8	10·523	9·745	8·745
9	10·728	10·358	9·877
10	11·936	11·301	10·485
11	12·274	11·713	10·992
12	14·675	13·612	12·246

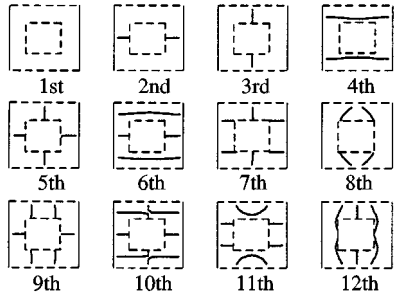

Figure 16. Nodal patterns for fsfs square plate with square hole.

6.2.5 *Fsfs square plate with circular hole*

Numerical solutions for the lowest 12 natural frequency parameters λ of fsfs square plate with a circular hole at the central part shown in Figure 6(h) are given in Table 8. The thickness ratio h_0/a of these plates is 0·01. The nodal patterns of the 12 modes of the plate are shown in Figure 16.

7. CONCLUSIONS

By adopting the view that plates with a hole can be considered ultimately as a kind of rectangular plates with non-uniform thickness, an approximate method was proposed for analyzing the free-vibration problem of rectangular plates with variously-shaped and arbitrary-located hole using the Green function of the equivalent rectangular plate with non-uniform thickness.

As a result of numerical work, it was shown that the numerical solutions obtained by the proposed method had good convergency and sufficient accuracy

for some examples of plates with a hole, and a lot of numerical data have been obtained.

REFERENCES

1. T. Kumai 1952 *Proceeding of second Japanese national congress of applied mechanics*, 339–342. The flexural vibrations of a square plate with a central hole.
2. S. Takahasi 1958 *Japanese society of mechanical engineers Bulletin* **1,** 380–385. Vibration of rectangular plates with circular holes.
3. C. V. Joga Rao and G. Pickett 1961 *Journal of the Aeronautical Society of India* **13**, 83–88. Vibrations of plates of irregular shapes and plates with holes.
4. P. Paramasivam 1973 *Journal of Sound and Vibration* **30**, 173–178. Free vibration of square plates with square openings.
5. R. F. Hegarty and T. Ariman 1975 *International Journal of Solids and Structures* **11**, 895–906. Elasto-dynamic analysis of rectangular plates with circular holes.
6. G. Aksu and R. Ali 1976 *Journal of Sound and Vibration* **44**, 147–158. Determination of dynamic characteristics of rectangular plates with cutouts using a finite difference formulation.
7. R. Ali and S. J. Atwal 1980 *Computers and Structures* **12**, 819–823. Prediction of natural frequencies of vibration of rectangular plates with rectangular cutouts.
8. J. N. Reddy 1982 *Journal of Sound and Vibration* **83**, 1–10. Large amplitude flexural vibration of layered composite plates with cutouts.
9. T. Sakiyama and M. Huang 1998 *Journal of Sound and Vibration* **216**, 379–397. Free vibration analysis of rectangular plates with variable thickness.
10. T. Sakiyama and H. Matsuda 1983 *Proceedings of Japan Society of Civil Engineers* **338**, 21–28. Bending analysis of rectangular plates with variable thickness.

APPENDIX A

$$F_{111} = F_{123} = F_{134} = F_{146} = F_{167} = F_{178} = F_{188} = 1,$$

$$F_{212} = F_{225} = F_{233} = F_{257} = F_{266} = \mu,$$

$$F_{156} = \nu, \quad F_{247} = \nu\mu, \quad F_{322} = F_{331} = -\mu, F_{344} = F_{355} = -I,$$

$$F_{363} = -J, F_{372} = -\kappa, F_{377} = 1, \quad F_{381} = -\mu\kappa,$$

$$F_{386} = \mu \quad \textit{other } F_{1te}, F_{2te}, F_{3te} = 0,$$

$$I = \mu(1-\nu^2)(h_0/h)^3, \quad J = 2\mu(1+\nu)(h_0/h)^3, \quad \kappa = (1/10)(E/G)(h_0/a)^2(h_0/h).$$

APPENDIX B

$$A_{p1} = \gamma_{p1}, \quad A_{p2} = 0, \quad A_{p3} = \gamma_{p2}, \quad A_{p4} = \gamma_{p3}, \quad A_{p5} = 0, \quad A_{p6} = \gamma_{p4} + \nu\gamma_{p5},$$

$$A_{p7} = \gamma_{p6},$$

$A_{p8}=\gamma_{p7}$, $B_{p1}=0$, $B_{p2}=\mu\gamma_{p1}$, $B_{p3}=\mu\gamma_{p3}$, $B_{p4}=0$, $B_{p5}=\mu\gamma_{p2}$ $B_{p6}=\mu\gamma_{p6}$,

$B_{p7}=\mu(v\gamma_{p4}+\gamma_{p5})$, $B_{p8}=\gamma_{p8}$, $C_{p1kl}=\mu(\gamma_{p3}+\kappa_{kl}\gamma_{p7})$, $C_{p2kl}=\mu\gamma_{p2}+\kappa_{kl}\gamma_{p8}$,

$C_{p3kl}=J_{kl}\gamma_{p6}$, $C_{p4kl}=I_{kl}\gamma_{p4}$, $C_{p5kl}=I_{kl}\gamma_{p5}$, $C_{p6kl}=-\mu\gamma_{p7}$, $C_{p7kl}=-\gamma_{p8}$,

$C_{p8kl}=0$, $[\gamma_{pk}]=[\bar{\gamma}_{pk}]^{-1}$, $\bar{\gamma}_{11}=\beta_{ii}$, $\bar{\gamma}_{12}=\mu\beta_{jj}$, $\bar{\gamma}_{22}=-\mu\beta_{ij}$,

$\bar{\gamma}_{23}=\beta_{ii}$, $\bar{\gamma}_{25}=\mu\beta_{jj}$,

$\bar{\gamma}_{31}=-\mu\beta_{ij}$, $\bar{\gamma}_{33}=\mu\beta_{jj}$, $\bar{\gamma}_{34}=\beta_{ii}$, $\bar{\gamma}_{44}=-I_{ij}\beta_{ij}$, $\bar{\gamma}_{46}=\beta_{ii}$, $\bar{\gamma}_{47}=\mu v\beta_{jj}$,

$\bar{\gamma}_{55}=-I_{ij}\beta_{ij}$,

$\bar{\gamma}_{56}=v\beta_{ii}$, $\bar{\gamma}_{57}=\mu\beta_{jj}$, $\bar{\gamma}_{63}=-J_{ij}\beta_{ij}$, $\bar{\gamma}_{66}=\mu\beta_{jj}$, $\bar{\gamma}_{67}=\beta_{ii}$,

$\bar{\gamma}_{71}=-\mu\kappa_{ij}\beta_{ij}$, $\bar{\gamma}_{76}=\mu\beta_{ij}$,

$\bar{\gamma}_{78}=\beta_{ii}$, $\bar{\gamma}_{82}=-\kappa_{ij}\beta_{ij}$, $\bar{\gamma}_{87}=\beta_{ij}$, $\bar{\gamma}_{88}=\beta_{jj}$, *other* $\bar{\gamma}_{pk}=0$, $\beta_{ij}=\beta_{ii}\beta_{jj}$.

APPENDIX C

$$a_{11i0i1}=a_{13i0i2}=a_{14i0i3}=a_{16i0i4}=a_{17i0i5}=a_{18i0i6}=1,\quad a_{15i0i3}=v,$$

$$a_{220jj1}=a_{230jj2}=a_{250jj3}=a_{260jj4}=a_{270jj5}=a_{280jj6}=1,\quad a_{240jj3}=v,\quad a_{230002}=0,$$

$$a_{hpijuv}=\sum_{e=1}^{8}\left\{\begin{array}{l}\displaystyle\sum_{k=0}^{i}\beta_{ik}A_{pe}[a_{hek0uv}-a_{hekjuv}(1-\delta_{ki})]+\sum_{l=0}^{j}\beta_{jl}B_{pe}[a_{he0luv}-a_{heiluv}(1-\delta_{lj})]\\ \displaystyle+\sum_{k=0}^{i}\sum_{l=0}^{j}\beta_{ik}\beta_{jl}C_{pekl}a_{hekluv}(1-\delta_{ki}\delta_{lj})\end{array}\right\},$$

where $h=1,2$, $p=1,2,\ldots,8$, $i=1,2,\ldots,m$, $j=1,2,\ldots,n$, $v=1,2,\ldots,6$, $u=0,1,\ldots,i$ $(h=1)$, $0,1,\ldots,j$ $(h=2)$,

$$\bar{q}_{pij}=\sum_{e=1}^{8}\left\{\begin{array}{l}\displaystyle\sum_{k=0}^{i}\beta_{ik}A_{pe}[\bar{q}_{ek0}-\bar{q}_{ekj}(1-\delta_{ki})]+\sum_{l=0}^{j}\beta_{jl}B_{pe}[\bar{q}_{e0l}-\bar{q}_{e1l}(1-\delta_{lj})]\\ \displaystyle+\sum_{k=0}^{i}\sum_{l=0}^{j}\beta_{ik}\beta_{jl}C_{pekl}\bar{q}_{ekl}(1-\delta_{kl}\delta_{lj})\end{array}\right\}$$
$$-\gamma_{p1}u_{1q}u_{jr}.$$